



# Declines in an abundant aquatic insect, the burrowing mayfly, across major North American waterways

Phillip M. Stepanian<sup>a,b,c,1</sup>, Sally A. Entekin<sup>d</sup>, Charlotte E. Wainwright<sup>e</sup>, Djordje Mirkovic<sup>e</sup>, Jennifer L. Tank<sup>f</sup>, and Jeffrey F. Kelly<sup>a,b</sup>

<sup>a</sup>Department of Biology, University of Oklahoma, Norman, OK 73019; <sup>b</sup>Corix Plains Institute, University of Oklahoma, Norman, OK 73019; <sup>c</sup>Department of Civil and Environmental Engineering and Earth Sciences, University of Notre Dame, Notre Dame, IN 46556; <sup>d</sup>Department of Entomology, Virginia Tech, Blacksburg, VA 24060; <sup>e</sup>Cooperative Institute for Mesoscale Meteorological Studies, University of Oklahoma, Norman, OK 73072; and <sup>f</sup>Department of Biological Sciences, University of Notre Dame, Notre Dame, IN 46556

Edited by David W. Schindler, University of Alberta, Edmonton, Canada, and approved December 12, 2019 (received for review August 6, 2019)

**Seasonal animal movement among disparate habitats is a fundamental mechanism by which energy, nutrients, and biomass are transported across ecotones. A dramatic example of such exchange is the annual emergence of mayfly swarms from freshwater benthic habitats, but their characterization at macroscales has remained impossible. We analyzed radar observations of mayfly emergence flights to quantify long-term changes in annual biomass transport along the Upper Mississippi River and Western Lake Erie Basin. A single emergence event can produce 87.9 billion mayflies, releasing 3,078.6 tons of biomass into the airspace over several hours, but in recent years, production across both waterways has declined by over 50%. As a primary prey source in aquatic and terrestrial ecosystems, these declines will impact higher trophic levels and environmental nutrient cycling.**

bioflow | ecotone | emergence | Ephemeroptera | radar entomology

**W**e have limited understanding of the critical link between ecosystem function and the phenology and magnitude of spatial flows of nutrients, energy, and organisms (1, 2), yet these flows are increasingly disrupted by anthropogenic environmental change with dynamic cascading effects on ecology and biogeochemistry (3). Modern remote-sensing techniques have enabled landscape-scale budgeting of plant and soil biomass, but the flow of organisms has been particularly difficult to quantify (3). Seasonal movements of animals drive community structure, ecosystem function, and connectivity through the transport and cycling of biomass and nutrients across space and time (4–7). Recent technological advances in animal monitoring have enabled some of the first quantitative descriptions of journeys undertaken by billions of individuals within aquatic, terrestrial, and aerial habitats, and these extremes in both number and spatial scale highlight the importance of animal movement in foundational environmental and ecological processes (5–11). Despite these advances, quantifying the magnitude of seasonal movements across aquatic, aerial, and terrestrial habitat interfaces in an ecosystem context remains problematic. Spanning the aquatic–terrestrial ecotone, the lifecycle of burrowing mayflies (*Hexagenia* spp.) is an extreme example of massive ecosystem fluxes with impacts on fundamental ecology, biogeochemical cycling, and human society.

Through the middle of the 20th century, enormous summertime swarms of *Hexagenia* mayflies were a common sight across many of North America's largest waterways. The immense scale of mayfly emergences made them a natural spectacle, and reports of the aquatic insects blanketing waterfront cities regularly filled newspaper headlines (12). Deep drifts of mayflies rendered streets impassable until snowplows could clear and grit roadways, and the dense swarms reduced visibility and inhibited water navigation, temporarily halting river transportation (12). These large *Hexagenia* populations were vital for supporting the commercial fishing industry and recreational anglers (13)

while also serving as a perennial annoyance for waterside residents; most of all, these mayfly emergences were a conspicuous sign of a productive, functional aquatic ecosystem (14–17). However, by 1970, these mass emergences had largely disappeared. The combination of increasing eutrophication from agricultural runoff, chronic hypoxia, hydrologic engineering, and environmental toxicity resulted in the disappearance of *Hexagenia* from many prominent midwestern waterways, with complete extirpation from the Western Lake Erie Basin and large segments of the Illinois, Ohio, and Mississippi Rivers (12–15, 17, 18). After two decades of absence, targeted efforts in conservation and environmental protection led to the eventual recovery of *Hexagenia* populations and recolonization of major habitats in the early 1990s (17, 18). Although the annual cycle of mayfly emergence has once more become commonplace in much of North America (Fig. 1), quantifying the ecological significance of these events at macroscales has remained impossible. Moreover, historical precedent shows that these large freshwater ecosystems are especially vulnerable to environmental change, making *Hexagenia* emergence an effective indicator of ecological “health” of waterways and motivating development of large-scale monitoring capabilities (14, 16).

We used weather surveillance radar to conduct nightly surveys of *Hexagenia* abundance over the Western Lake Erie Basin

## Significance

**The annual appearance of massive mayfly swarms is a source of public fascination and spectacular natural phenomenon that plays a key role in regional food webs. Alarming reports of insect declines motivate efforts to uncover long-term and large-scale invertebrate population trends. Monitoring aquatic insect abundance across ecosystems continues to be logistically infeasible, leaving the vulnerability of these communities to intensifying anthropogenic impacts unknown. We apply radar remote sensing to quantify aquatic insect abundance at scales that have been previously impossible, revealing persistent declines in biomass flux from aquatic to terrestrial habitats. As ecological indicators, these losses may signal deterioration in water quality and, if current population trends continue, could cascade to widespread disappearance from some of North America's largest waterways.**

Author contributions: P.M.S. and C.E.W. designed research; P.M.S. performed research; D.M. contributed new reagents/analytic tools; P.M.S. analyzed data; and P.M.S., S.A.E., C.E.W., J.L.T., and J.F.K. wrote the paper.

The authors declare no competing interest.

This article is a PNAS Direct Submission.

Published under the PNAS license.

<sup>1</sup>To whom correspondence may be addressed. Email: p.step@nd.edu.

This article contains supporting information online at <https://www.pnas.org/lookup/suppl/doi:10.1073/pnas.1913598117/-DCSupplemental>.

First published January 21, 2020.

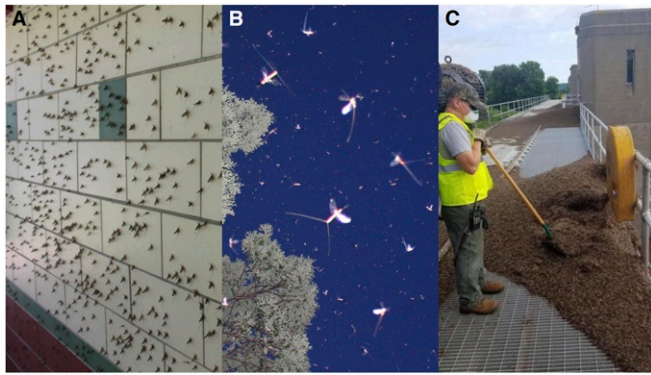


**Fig. 1.** Local-scale phenomenology of a *Hexagenia* mayfly emergence. (A) Following up to 2 y of growth as an aquatic nymph, mayflies ascend to the water surface en masse, molt into a volant subadult form, and fly to sheltered land to undergo a second molt. These dusk emergence flights result in dense waves of subadults that blanket shorelines. (B) The mayflies spend the following day molting into their sexually mature adult form, taking flight at sunset to engage in spectacular mating swarms that are followed quickly by oviposition and death. (C) Within 2 d of the initial emergence, tons of dead mayflies litter the shoreline, resulting in a substantial biomass flux to the surrounding terrestrial environment. Image courtesy of Jeff Ferguson/U.S. Army Corps of Engineers.

and Upper Mississippi River and investigate patterns in emergence magnitude across these two iconic waterbodies over time. Just as radar remote sensing has been used to quantify long-term changes in the abundance of migratory organisms in flight (i.e., birds (10, 11), insects (8, 9), and bats (19)), we exploit

*Hexagenia*'s synchronous aerial emergences to quantify the flux of these benthic organisms across the water–air interface and produce a long-term time series of changes in system-wide abundance (*Materials and Methods*). This application of macroscale remote sensing provides a phenomenological perspective of these synchronized emergences, demonstrating the regional extent of mayfly abundance, dispersal, and deposition (Fig. 2). Moreover, this expanded capacity to make quantitative long-term measurements of macrobenthos that engage in synchronized mass emergence flights offers a regional view of the effects of environmental change on emergence phenomena, a key aspect of aquatic insect ecology (Figs. 3 and 4).

## Results

Total annual bioflux of *Hexagenia* mayflies occurs in several episodic emergence events, each occurring over an isolated geographical extent and demonstrating a unique phenology that is likely associated with distinct benthic thermal regimes and abiotic cues (20, 21). The largest emergence events in Lake Erie occur over the center of the western basin and can result in a flux of up to 87.9 billion mayflies (3,078.6 tons of biomass) across the water–air interface in a single night. A 697-km stretch of the Upper Mississippi River can produce up to 3.25 billion individuals (114 tons) in one evening. Accumulating this productivity over the emergence season, annual aquatic–terrestrial bioflux represents the total biomass transported from benthic habitats through the airspace into terrestrial ecosystems. Annual *Hexagenia* bioflux over the western basin of Lake Erie can exceed 115 billion individuals (4,031 tons;  $2.19 \text{ g m}^{-2} \text{ y}^{-1}$ ,  $0.94 \text{ g C m}^{-2} \text{ y}^{-1}$ ,  $0.22 \text{ g N m}^{-2} \text{ y}^{-1}$ ,  $0.01 \text{ g P m}^{-2} \text{ y}^{-1}$ ), while the Upper Mississippi River produces up to 20.5 billion mayflies annually,

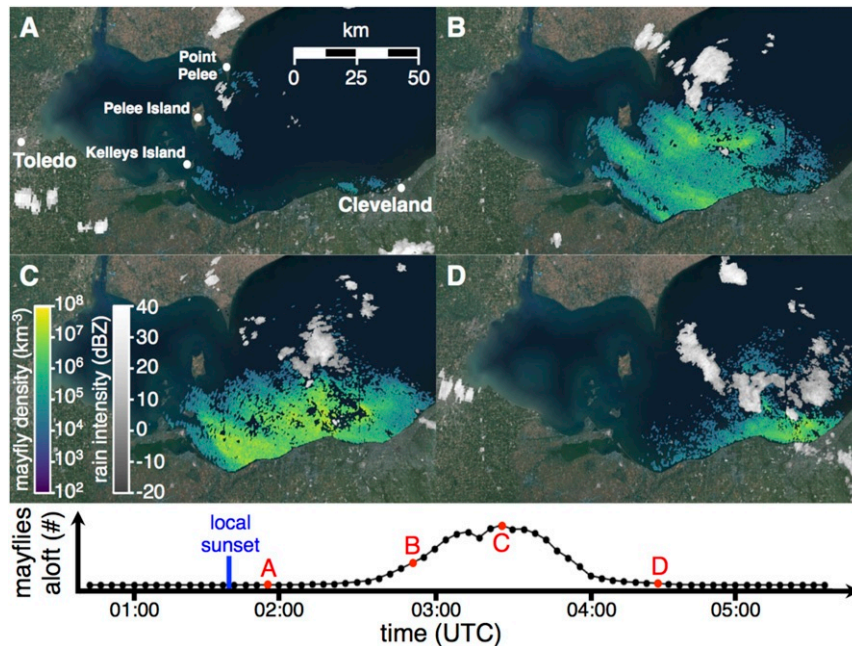


**Fig. 2.** Macroscale phenomenology of a mayfly emergence over Lake Erie on the night of June 27, 2018 as observed by weather surveillance radar. (A) Radar snapshot at 01:56 Coordinated Universal Time (UTC) depicting the initial ascent of mayflies from the lake surface surrounding the shorelines of Point Pelee, Pelee Island, and Kelleys Island. At this time, a total of 2.1 million mayflies are detected in the airspace. (B) Radar snapshot at 02:50 UTC showing the continuing ascent and downwind drift of mayflies across the lake to the southeast. Additional emerging mayfly plumes develop surrounding North, Middle, and South Bass Islands. Mayflies reaching the southern lakeshore rapidly descend out of the airspace. At this time, a total of 394 million mayflies are detected in the airspace. (C) Radar snapshot at 03:32 UTC. Emergence and ascent have largely terminated as mayflies continue to fly downwind toward the southern lakeshore. At this time, the aerial abundance reaches a maximum, with a total of 2.0 billion mayflies detected in the airspace. (D) Radar snapshot at 04:32 UTC. Most mayflies have already descended from the airspace as the trailing edge of the mayfly plume approaches the southern lakeshore. At this time, a total of 81 million mayflies are detected in the airspace. (Lower) The time series of aerial mayfly abundance during the emergence event. The mayfly numbers given in A–D are annotated as well as the time of local sunset. The full radar loop of this emergence event is provided as [Movie S1](#).

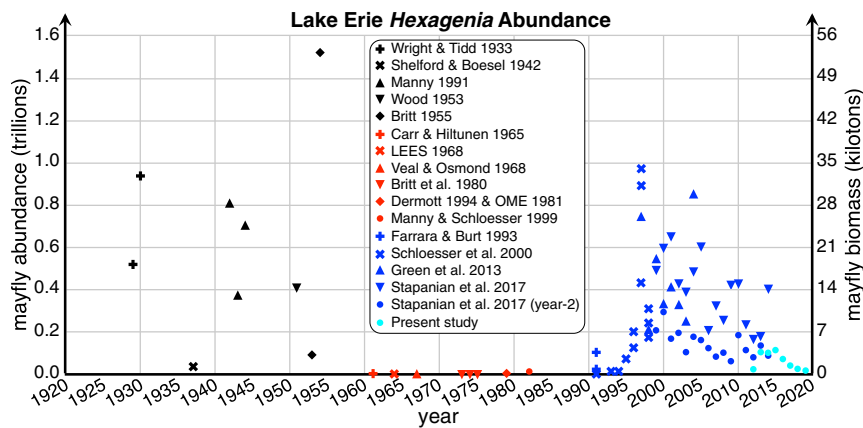


**Fig. 3.** Long-term variability in *Hexagenia* mayfly abundance (individuals  $\times 10^{12}$ ) and biomass (tons  $\times 10^3$ ) in the Western Lake Erie Basin. Historical estimates of total *Hexagenia* abundance are derived from benthic sampling of nymph densities prior to (black), during (red), and after (blue) extirpation (*Materials and Methods*) as well as directly by radar surveys of emerging subimagoes (cyan). Considering the required 2-y developmental period for a *Hexagenia* nymph to reach maturity, radar emergence surveys (cyan) should be most comparable with the abundance of year 2 nymphs (blue circles). Refs. 15, 17, 18, and 49–61 have details on benthic sampling procedures in the referenced studies.

resulting in an aquatic–terrestrial flux of 720 tons of biomass (emergent biomass per area:  $1.88 \text{ g m}^{-2}$ ; emergent biomass per length river shoreline:  $1.03 \text{ kg m}^{-1} \text{ y}^{-1}$ ,  $446.7 \text{ g C m}^{-1} \text{ y}^{-1}$ ,  $111.11 \text{ g N m}^{-1} \text{ y}^{-1}$ ,  $3.6 \text{ g P m}^{-1} \text{ y}^{-1}$ ).

Aquatic insect emergence can play a substantial role in nutrient transport to surrounding terrestrial ecosystems (22), and within these two waterways, annual *Hexagenia* emergences can translocate as much as 475 tons of nitrogen and 16 tons of phosphorus across ecotones. For context, the phosphorus removed from the Western Lake Erie Basin in 1 y through *Hexagenia* emergence offsets one-third of the annual soluble reactive phosphorus loading to the basin through atmospheric deposition (*Materials and Methods*). These movements also serve as a massive resource pulse for surrounding terrestrial trophic systems (2), and the abundance of volant aquatic insects, in particular, has been linked to fledging success in insectivorous birds (23, 24). Annual *Hexagenia* emergence in the Western Lake Erie Basin can export up to 12 trillion calories of food resources—enough to support the energetic demands of over 53 million nestling birds from hatching to fledging (*Materials and Methods*). As a basis for comparison, the magnitude of aquatic–terrestrial biomass transport during *Hexagenia* emergences can be orders of magnitude greater than bioflows of migratory terrestrial insects (e.g.,  $0.046 \text{ g m}^{-2} \text{ y}^{-1}$ ) (8) and approaching the mass flux of

migrating birds (e.g.,  $72.5 \text{ kg m}^{-1} \text{ y}^{-1}$ ) (11), demonstrating their significant contribution to resource subsidies.

Although we are just now quantifying the extent to which *Hexagenia* emergences contribute to ecological processes, it is already clear that this phenomenon is undergoing rapid change. Less than a decade after the recolonization of *Hexagenia* in Lake Erie, populations have begun exhibiting chronic declines punctuated by acute fluctuations in abundance (Fig. 3) (17). In the period from 2015 to 2019, radar surveys indicated an 84% decrease in *Hexagenia* abundance, corroborating trends from localized benthic sampling of nymphs (17). This pattern of decline holds true for the Upper Mississippi River as well, which showed a decrease of 52% from 2012 to 2019 (Fig. 4).

## Discussion

Aquatic insect emergence is an effective mechanism for rapidly transporting enormous pulses of biomass across ecotones, with direct ecological influences ranging from environmental nutrient cycling (22) to animal behavior (23). Annual *Hexagenia* emergences represent the exchange of hundreds of tons of elemental nutrients, thousands of tons of biomass, billions of organisms, and trillions of calories worth of energy to the surrounding terrestrial habitat. While radar surveillance can quantify insect emergence and aerial drift, the ultimate fate of these materials

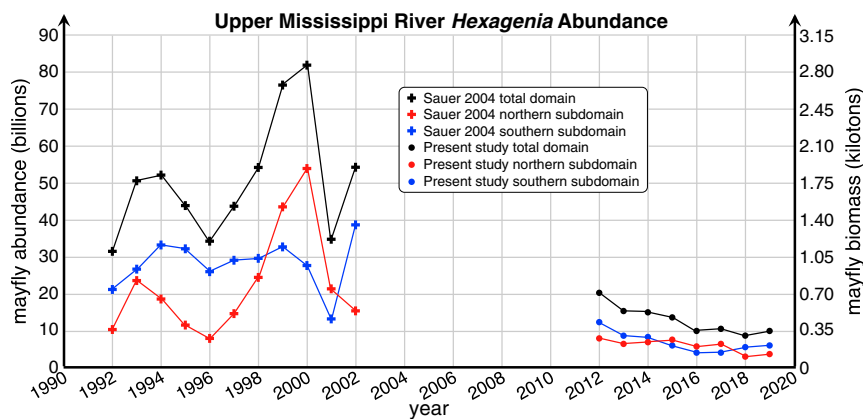


**Fig. 4.** Ongoing declines in *Hexagenia* mayfly abundance (individuals  $\times 10^9$ ) and biomass (tons  $\times 10^3$ ) on the Upper Mississippi River. Surveys of *Hexagenia* abundance over the Upper Mississippi River (black) as well as contributions from the northern (La Crosse, WI; red) and southern (Davenport, IA; blue) subdomains as measured by benthic sampling (crosses) (62) and radar surveillance (circles).

is often subject to the effects of human influence (e.g., large-scale removal efforts) (Fig. 1C). Especially for the midwestern water bodies considered, it is difficult to contextualize the effect of *Hexagenia* emergence separate from related human activities. For example, although the export of phosphorus from water bodies by *Hexagenia* emergence may be of similar magnitude to some natural inputs, when considering current contributions from anthropogenically enhanced inputs (e.g., industrial point sources and agricultural runoff), phosphorus exports represent less than 1% of total annual loading. It is possible that, prior to the onset of industrial agriculture, aquatic insect emergence may have been a significant mechanism for offsetting phosphorus inputs from natural sources; presently, however, anthropogenic loadings to these specific water bodies make these emergent nutrient exports virtually negligible to the overall budget.

Although humans contribute heavily to nitrogen and phosphorus cycling in midwestern waterways, these nutrient contributions are not available across all trophic levels, making insect emergence a major nutritional source for terrestrial predators and scavengers (2, 23, 24). Seasonal pulses of volant aquatic insects are especially important to avian aerial insectivores, which synchronize their breeding phenology to correspond with emergence and rely on these high-quality food sources for fledgling success (23). In this regard, reports of significant declines in aerial insectivore populations across North America have been partially tied to the availability of insect prey (25) and in particular, emerging aquatic insects (23, 24).

We have found persistent declines in *Hexagenia* abundance within Lake Erie and the Mississippi River. Similar trends across both lentic and lotic waterways suggest the pervasive effect of multiple anthropogenic stressors on freshwater ecosystems. These ongoing reductions in *Hexagenia* populations may offer a window to the near-future environmental and ecological changes throughout these waterways. As the climate continues to warm, lake stratification between June and September will become more common (26), leading to decreased benthic oxygen concentrations, chronic hypoxia, and emergence failures (27). Warmer surface waters fed by phosphorus-rich spring runoff into Lake Erie will continue to trigger summer algae blooms, releasing toxins, such as microcystin, into the environment (28). *Hexagenia* are highly sensitive to these toxins (29), and as algae blooms become more expansive and frequent in regions already susceptible to hypoxia, emergence failures are more likely to occur. At the same time, nutrient-laden runoff will continue to increase lake turbidity and orthophosphates that promote hypoxic conditions by driving oxygen concentrations lower and for longer (30). Compounding the effects of hypoxia and toxicity, pesticide concentrations are increasing in freshwater ecosystems. Neonicotinoid concentrations in Great Lake tributaries can be up to 40 times greater than the Chronic Concentration set by US Environmental Protection Agency Aquatic Life Benchmark (31), and *Hexagenia* are among the most sensitive aquatic insects to a suite of these commonly applied pesticides. Even at sub-lethal levels, the presence of neonicotinoids will lead to greater susceptibility to hypoxia, reduced fitness, and increased predation (32). Exacerbating these effects, pesticide concentrations in sediment can be even greater than in the overlying water (33), and as detritivores, *Hexagenia* nymphs will experience two pathways of increasing pesticide exposure: dissolved in water and stored in sediment. Taken as a whole, multiple interacting threats to aquatic insects may present the possibility of once again extirpating *Hexagenia* from these waterways.

Persisting global declines in insect abundance have flooded public awareness and have led to speculation of so-called “Ecological Armageddon” scenarios in the near future (34, 35). There is a critical need to objectively inform these dialogues, but quantitative monitoring of insect systems is logistically challenging

and can be subject to bias (35, 36). Long-term radar measurements are an emerging tool for substantiating magnitudes and rates of regional declines of insect biomass. Moreover, radar measurements can extend exploration of these themes to benthic ecotones, providing the first spatially comprehensive, regional assessments of aquatic insect population declines. This technique holds the potential of providing standardized sampling in other parts of the world (e.g., Africa) (37) and may be used to monitor population trends in other aquatic insects that emerge in large numbers, such as caddisflies and midges. As a vital prey source for insectivores, *Hexagenia* declines undoubtedly impact trophic structure of surrounding ecosystems. Our results suggest a widespread and multiyear decline in the populations of mayflies in the American Midwest. These patterns contribute a spatiotemporal perspective to existing data and further motivate examination of the changing water quality of the Great Lakes region, with particular interest in interactions among water temperature, nutrient runoff, and pesticides. If these population trends continue, persistent environmental changes could threaten to once more extirpate *Hexagenia* mayflies from North America’s largest waterways, making this ephemeral spectacle—and its vital ecological functions—a thing of the past.

## Materials and Methods

The US National Weather Service operates a network of weather surveillance radars (NEXRAD, hereafter) that provides continuous, high-resolution measurements of the national airspace. Although this system was deployed with the mission of improving weather prediction and analysis, a beneficial by-product has been the capacity to systematically monitor aerial wildlife (e.g., birds, bats, and insects) (38). Background information on radar theory and operation, specifically focusing on ecological applications of NEXRAD, has been compiled in several primers (38–40). Among the phenomena routinely detected by radar, regional emergences of aquatic insects have been repeatedly documented over several waterways and validated by visual ground observations. By far, the most prolific of these emergences are the annual flights of burrowing mayflies (*Hexagenia* spp.) on the Upper Mississippi River and Western Lake Erie Basin, both of which regularly garner widespread media coverage. It is because of the high confidence in species composition making up these emergence events that we chose to focus analysis on these two waterways.

**Weather Radar System Specifications and Site Descriptions.** Our analysis domain on the Upper Mississippi River spans a 697-km stretch from Lock 3 to Lock 19 and includes a 10-km buffer extending outward from the river. The combined surveillance area of two weather radars covers the entirety of this domain. The first radar is located at the National Weather Service office in La Crosse, Wisconsin (International Civil Aviation Organization site identifier: KARX) and transmits at a frequency of 2,770 MHz (wavelength: 10.82 cm). The KARX radar location (43.8228°N, 91.1911°W, 413.6 m above mean sea level [AMSL]) provides coverage of the upper segment of the analysis domain, north of the 42.67°N parallel. Dual-polarization radar measurements at the KARX site began on 15 April 2012. The second radar is located at the National Weather Service office in Davenport, Iowa (International Civil Aviation Organization site identifier: KDVN) and transmits at a frequency of 2,860 MHz (wavelength: 10.48 cm). The KDVN radar location (41.6116°N 90.5810°W, 259.4 m AMSL) provides coverage of the lower segment of the analysis domain, south of the 42.67°N parallel. Dual-polarization radar measurements at the KDVN site began on 23 March 2012. Our analysis domain on Lake Erie covers the western and central basins and is surveyed by the radar located at the National Weather Service office in Cleveland, Ohio (International Civil Aviation Organization site identifier: KCLE). The KCLE radar transmits at a frequency of 2,875 MHz (wavelength: 10.43 cm) and is positioned on the southern lakeshore (41.4131°N, 81.8597°W, 262.1 m AMSL). Dual-polarization radar measurements at the KCLE site began on 7 December 2011.

**Radar Data Access and Processing.** The full dataset of historical NEXRAD measurements is archived on the Amazon Web Services cloud and is continually appended with current measurements in real time. This dataset is open access and available for download online (41). We constrained our

analysis to the period during which dual-polarization measurements were available at the three radar sites (i.e., spring 2012 through present). Based on the known phenology of *Hexagenia* emergences on these waterways (typically occurring in early July), we defined our emergence season as 1 June through 15 August. This analysis window also served to avoid biomass contributions from other taxa with earlier emergence phenology (e.g., chironomid midges). For each day in this period, we found the time of local civil twilight (using the Python PyEphem package) and downloaded the radar volume scans from 1 h before to 4 h after civil twilight (using the Python Boto3 package). Each radar volume scan was read into Python using the Py-ART package (42) and processed following the workflow described in ref. 19 with the following modifications. First, all meteorological signals were identified and removed using the polarimetric methods described in ref. 43 by applying their depolarization ratio threshold of  $-12.5$  dB and reflectivity factor threshold of 45 dBZ. Second, all pixels outside of the spatial analysis domains described in the previous section (i.e., outside of the 10-km river buffer and outside of the lake) were removed. Third, all pixels having differential reflectivity less than 5 dB were removed to avoid contamination from migrating birds at the ends of the emergence season. Fourth, because mayflies should not be present at high altitudes, all sweeps above the  $2^\circ$  elevation angle were removed from the analysis to speed up computations. Finally, the resulting field of classified mayfly signals was despeckled using a  $3 \times 3$  structuring element following ref. 43. As in ref. 19, the volume of airspace sampled was calculated from beam geometry (units: kilometers<sup>3</sup>) and multiplied by the corresponding radar reflectivity (units: centimeters<sup>2</sup> kilometers<sup>-3</sup>) to obtain the backscattering area present in the radar sample (units: centimeters<sup>2</sup>). The backscattering area from the entire radar domain was summed (units: centimeters<sup>2</sup>) and divided by the radar cross-section of an individual mayfly (0.00179 cm<sup>2</sup> per individual; method is described in the following subsection). The final result is the estimated total number of individual mayflies aloft in the domain during the snapshot captured in the radar volume scan (Fig. 2, Lower).

#### Calculating *Hexagenia* Radar Cross-Section from Electromagnetic Modeling.

The method of moments as implemented in the WIPL-D software package has been shown to be an effective electromagnetic modeling technique for predicting the radar cross-sections of biota at radar frequencies (44, 45). Following the methods described in ref. 44, we created an equimass prolate ellipsoid model of a *Hexagenia* mayfly using a mass of 0.035 g (46), length-to-width ratio of 8.8246, length-to-height ratio of 10.2391, and dielectric permittivity of 42.8 to 15.21 (Lesser Grain Borer at 2.47 GHz obtained from table 5 in ref. 47). Radar cross-sections at the horizontal polarization were calculated at S band (2.86 GHz) for elevation angles spanning 0 through  $-2^\circ$  and across the full set of 360 azimuth angles (i.e., aspects representative of the radar observations). The mean radar cross-section over these aspects (0.00179 cm<sup>2</sup>) was taken to be the most representative value for quantifying the number of individual mayflies.

#### Estimating Nightly Mayfly Abundance and Annual Productivity from Radar Estimates.

As a result of the radar processing workflow, each radar volume scan has been converted into an instantaneous snapshot of the number of mayflies observed aloft (Fig. 2, Lower). To avoid double counting individuals in subsequent volume scans, we define the mayfly abundance for a given night as the single highest number of mayflies observed in the airspace during the emergence (e.g., the maximum value in Fig. 2, Lower). This metric is inherently an underestimate of total abundance because not all individuals are in the airspace simultaneously nor do all fly at sufficiently high altitudes to enter the radar beam. As a result, our abundance estimates represent the minimum number of individuals present. After obtaining an abundance estimate for each night, we sum all estimates over the season to find the accumulated annual mayfly productivity.

#### Converting from Individuals to Biomass, Bioflux, and Elemental Composition.

As described previously, the measuring unit associated with radar measures of abundance is number of individuals. To convert the number of individuals to biomass, we multiply by the mass of an average individual *Hexagenia* mayfly (0.035 g) (46) such that 115,165,486,290 individuals become 4,030,792,020 g or 4,031 metric tons. To reach units of annual flux as presented in ref. 1 (grams meter<sup>-2</sup> y<sup>-1</sup>), we divide the annual mass flux (e.g., 4,030,792,020 g in 2015 over Lake Erie) by the mayfly production area of Lake Erie (1,840 km<sup>2</sup>) (15) to yield  $2.19$  g m<sup>-2</sup> y<sup>-1</sup>. We take the same approach over the Mississippi River to convert into flux units over the mayfly production area of the river as in ref. 15 (grams meter<sup>-2</sup> using 50% of northern [411,445,932 m<sup>2</sup>] and southern [353,425,712 m<sup>2</sup>] subdomain areas)

as well as along the shoreline as presented in ref. 2 (grams meter<sup>-1</sup> y<sup>-1</sup>). For example, the total annual mayfly production in 2012 (2.05835178e10 individuals y<sup>-1</sup>) is converted to biomass (720,423,123 g y<sup>-1</sup>) and divided by the length of the river analysis domain (697 km) to reach the final flux units (1.0336 kg m<sup>-1</sup> y<sup>-1</sup>). We apply this same approach for calculating the annual flux of high-altitude insect migrants (8) by dividing biomass (3,200 tons y<sup>-1</sup>) by passage area (70,000 km<sup>2</sup>) to obtain the proper units (0.04571 g m<sup>-2</sup> y<sup>-1</sup>). Similarly, for migrating birds with an average mass of 50 g (11), we considered the annual fall (3.97 billion birds) and spring (2.56 billion birds) passage over a 4,503.22-km transect along the northern United States, resulting in a passage flux of 72.5 kg m<sup>-1</sup> y<sup>-1</sup>. Finally, we converted *Hexagenia* biomass and bioflux to elemental contributions of carbon, nitrogen, and phosphorus to demonstrate the subsidy to prey. Values of *Hexagenia* carbon (43%), nitrogen (10%), and phosphorus (0.35%) are from upper Midwest US populations (48).

**Benthic Sampling and Historical Abundance Estimation.** The benthic samples shown in Fig. 3 represent a literature review of historical estimates of *Hexagenia* nymph densities obtained by dredge and grab sample surveys throughout Western Lake Erie Basin (15, 17, 18, 49–61). These studies present nymph abundance in terms of benthic density using units of nymphs per square meter of lake bottom, with multiple samples typically taken across a variety of sites. Each point in Fig. 3 represents a single study season—the average of all site samples within a given study and season—for the given year. As such, if multiple studies took samples during the same year or if samples were taken across several seasons within a year, these cases result in multiple unique study season points for that year. With the exception of ref. 17, all studies present the total density of all *Hexagenia* nymphs within the sample. One study (17) further identified nymphs to age class, and we plotted both the total *Hexagenia* nymph density (Fig. 3, blue downward-pointing triangles) consistent with all other benthic surveys as well as the density of year 2 age class nymphs (Fig. 3, blue circles). Following a 2-y development cycle from egg to emergence, we expect that the abundance of year 2 nymphs should be more representative of the abundance of emerging subimagos surveyed by radar. Finally, we follow the method presented in ref. 15 to scale nymph densities to full basin abundance by multiplying densities by the habitable benthic area of the Western Lake Erie Basin. Full details of the sites, dates, and sampling strategies appearing in Fig. 3 can be found in refs. 15, 17, 18 and 49–61. This same approach was taken for benthic samples on pools 8 and 13 of the Mississippi River (62) scaled as in ref. 15 using 50% of the benthic surface area of the northern and southern subdomains, respectively.

**Lake Erie Phosphorus Budget Calculations.** We obtained the most recent estimates (2013) of soluble reactive phosphorus inputs to the Western Lake Erie Basin summed with inflow contributions from Lake Huron from the data tables presented in ref. 63. We took the annual soluble reactive phosphorus from atmospheric deposition (39 tons in 2013) as well as the 2013 total input including all sources (1,732 tons). We compared these input values with the phosphorus export from the Western Lake Erie Basin from *Hexagenia* emergence in 2013 (12.86 tons) to find the percentage of phosphorus export with respect to input mass (i.e., 33% of atmospheric deposition and 0.74% of total inputs).

***Hexagenia* Energetic Calculations.** Starting with the 104.49 calories contained in a single *Hexagenia limbata* (64), we multiply by the Lake Erie emergence (115 billion individuals) to get annual caloric content (12.016 trillion calories). We took the tree swallow (*Tachycineta bicolor*) as a model aerial insectivore that has been shown to rely on aquatic insect emergence for feeding fledglings during the nesting season (23, 24). Dividing the total annual caloric content of the emergence (12.016 billion kcal) by the required 224 kcal to raise a nestling over the 15-d development period (65), we arrive at the total number of nestlings that can be supported by this food resource (53.6 million birds).

#### Data Availability.

The full dataset of NEXRAD radar measurements used in this analysis is open access and archived on the Amazon Web Services cloud (41).

**ACKNOWLEDGMENTS.** We thank M. Steingraeber, E. Posthumus, D. Baumgardt, J. Sullivan, R. Haro, and M. Knutson for discussions on mayfly phenology and C. C. Vaughn for commenting on an early draft of the manuscript. This research was supported by NSF–Division of Emerging Frontiers Grant 1840230 and NSF–Division of Graduate Education Grant 1545261.

1. I. Gounand, C. J. Little, E. Harvey, F. Altermatt, Cross-ecosystem carbon flows connecting ecosystems worldwide. *Nat. Commun.* **9**, 4825 (2018).
2. D. M. Walters, J. S. Wesner, R. E. Zuellig, D. A. Kowalski, M. C. Kondratieff, Holy flux: Spatial and temporal variation in massive pulses of emerging insect biomass from western U.S. Rivers. *Ecology* **99**, 238–240 (2018).
3. O. J. Schmitz *et al.*, Animals and the zoogeochemistry of the carbon cycle. *Science* **362**, eaar3213 (2018).
4. R. Nathan *et al.*, A movement ecology paradigm for unifying organismal movement research. *Proc. Natl. Acad. Sci. U.S.A.* **105**, 19052–19059 (2008).
5. S. Bauer, B. J. Hoye, Migratory animals couple biodiversity and ecosystem functioning worldwide. *Science* **344**, 1242552 (2014).
6. N. E. Hussey *et al.*, Aquatic animal telemetry: A panoramic window into the underwater world. *Science* **348**, 1255642 (2015).
7. R. Kays, M. C. Crofoot, W. Jetz, M. Wikelski, Terrestrial animal tracking as an eye on life and planet. *Science* **348**, aaa2478 (2015).
8. G. Hu *et al.*, Mass seasonal bioflows of high-flying insect migrants. *Science* **354**, 1584–1587 (2016).
9. J. W. Chapman *et al.*, Flight orientation behaviors promote optimal migration trajectories in high-flying insects. *Science* **327**, 682–685 (2010).
10. B. M. Van Doren, K. G. Horton, A continental system for forecasting bird migration. *Science* **361**, 1115–1118 (2018).
11. A. M. Dokter *et al.*, Seasonal abundance and survival of north America's migratory avifauna determined by weather radar. *Nat. Ecol. Evol.* **2**, 1603–1609 (2018).
12. C. R. Fremling, Documentation of a mass emergence of hexagenia mayflies from the Upper Mississippi River. *Trans. Amer. Fish. Soc.* **4**, 373–398 (1994).
13. J. S. Schaeffer, J. S. Diana, R. C. Haas, Effects of long-term changes in the benthic community on yellow perch in Saginaw Bay, Lake Huron. *J. Great Lakes Res.* **23**, 340–351 (2000).
14. T. B. Reynoldson, D. W. Schloesser, B. A. Manny, Development of a benthic invertebrate objective for mesotrophic great lakes waters. *J. Great Lakes Res.* **97**, 278–281 (1968).
15. B. A. Manny, Burrowing mayfly nymphs in Western Lake Erie, 1942–1944. *J. Great Lakes Res.* **17**, 517–521 (1991).
16. J. K. Jackson, L. Füreder, Long-term studies of freshwater macroinvertebrates: A review of the frequency, duration and ecological significance. *Freshwater Biol.* **51**, 591–603 (2006).
17. M. A. Stapanian, P. M. Kočovský, B. L. Bodamer Scarbro, Evaluating factors driving population densities of mayfly nymphs in western Lake Erie. *J. Great Lakes Res.* **43**, 1111–1118 (2017).
18. D. W. Schloesser, K. A. Krieger, J. J. H. Ciborowski, L. D. Corkum, Recolonization and possible recovery of burrowing mayflies (Ephemeroptera: Ephemeridae: Hexagenia spp.) in Lake Erie of the Laurentian Great Lakes. *J. Aquat. Ecosyst. Stress Recovery* **8**, 125–141 (2000).
19. P. M. Stepanian, C. E. Wainwright, Ongoing changes in migration phenology and winter residency at bracken bat cave. *Glob. Change Biol.* **44**, 3266–3275 (2018).
20. D. W. Schloesser, K. A. Krieger, J. J. H. Ciborowski, L. D. Corkum, Timing of hexagenia (Ephemeroptera: Ephemeridae) mayfly swarms. *Can. J. Zool.* **84**, 1616–1622 (2006).
21. L. L. Wright, J. S. Mattice, Emergence patterns of Hexagenia bilineata: Integration of laboratory and field data. *Freshw. Invertebr. Biol.* **4**, 109–124 (1985).
22. J. Dreyer *et al.*, Quantifying aquatic insect deposition from lake to land. *Ecology* **96**, 499–509 (2015).
23. C. Wingfield Twining, J. Ryan Shipley, D. W. Winkler, Aquatic insects rich in omega-3 fatty acids drive breeding success in a widespread bird. *Ecol. Lett.* **21**, 1812–1820 (2018).
24. C. W. Twining *et al.*, Aquatic and terrestrial resources are not nutritionally reciprocal for consumers. *Funct. Ecol.* **33**, 2042–2052 (2019).
25. K. J. Spiller, R. Dettmers, Evidence for multiple drivers of aerial insectivore declines in north America. *Condor* **121**, duz010 (2019).
26. L. D. Mortsch, F. H. Quinn, Climate change scenarios for Great Lakes basin ecosystem studies. *Limnol. Oceanogr.* **4**, 373–398 (1994).
27. T. B. Bridgeman, D. W. Schloesser, A. E. Krause, Recruitment of Hexagenia mayfly nymphs in Western Lake Erie linked to environmental variability. *Ecol. Appl.* **16**, 601–611 (2006).
28. A. M. Michalak *et al.*, Record-setting algal bloom in Lake Erie caused by agricultural and meteorological trends consistent with expected future conditions. *Proc. Natl. Acad. Sci. U.S.A.* **110**, 6448–6452 (2011).
29. J. L. Smith, G. L. Boyer, E. Mills, K. L. Schulz, Toxicity of microcystin-LR, a cyanobacterial toxin, to multiple life stages of the burrowing mayfly, Hexagenia, and possible implications for recruitment. *Environ. Toxicol.* **23**, 499–506 (2008).
30. N. C. Everall, M. F. Johnson, P. Wood, L. Mattingley, Sensitivity of the early life stages of a mayfly to fine sediment and orthophosphate levels. *Environ. Pollut.* **237**, 792–802 (2018).
31. M. L. Hladik *et al.*, Year-round presence of neonicotinoid insecticides in tributaries to the Great Lakes, USA. *Environ. Pollut.* **235**, 1022–1029 (2018).
32. A. J. Bartlett *et al.*, Lethal and sublethal toxicity of neonicotinoid and butenolide insecticides to the mayfly, Hexagenia spp. *Environ. Pollut.* **238**, 63–75 (2018).
33. L. Hunt *et al.*, Insecticide concentrations in stream sediments of soy production regions of South America. *Sci. Total Environ.* **547**, 114–124 (2016).
34. C. A. Hallmann *et al.*, More than 75 percent decline over 27 years in total flying insect biomass in protected areas. *PLoS One* **12**, e0185809 (2017).
35. S. R. Leather, "Ecological armageddon"—more evidence for the drastic decline in insect numbers. *Ann. Appl. Biol.* **172**, 1–3 (2018).
36. B. I. Simmons *et al.*, Worldwide insect declines: An important message, but interpret with caution. *Ecol. Evol.* **9**, 3678–3680 (2019).
37. D. R. Reynolds, J. R. Riley, Radar observations of concentrations of insects above a river in Mali, West Africa. *Ecol. Entomol.* **4**, 161–174 (1979).
38. P. M. Stepanian, K. G. Horton, V. M. Melnikov, D. S. Zrnić, S. A. Gauthreaux Jr., Dual-polarization radar products for biological applications. *Ecosphere* **7**, e01539 (2017).
39. R. H. Diehl, R. P. Larkin, "Introduction to the WSR-88D (NEXRAD) for ornithological research" in *Bird Conservation Implementation and Integration in the Americas: Proceedings of the Third International Partners in Flight Conference*, C. J. Ralph, T. D. Rich, Eds. (US Department of Agriculture, Forest Service, Pacific Southwest Research Station, Albany, CA, 2005), pp. 876–888.
40. R. P. Larkin, R. H. Diehl, "Radar techniques for wildlife research" in *The Wildlife Techniques Manual*, N. J. Silvy, Ed. (The Johns Hopkins University Press, Baltimore, MD, ed. 7, 2012), pp. 319–335.
41. Amazon Web Services, NEXRAD on AWS. <https://s3.amazonaws.com/noaa-nexrad-level2/index.html>. Accessed 1 July 2019.
42. J. J. Helmus, S. M. Collis, The Python ARM Radar Toolkit (Py-ART), a library for working with weather radar data in the Python programming language. *J. Open Res. Softw.* **4**, e25 (2016).
43. A. Kilambi, F. Fabry, V. Meunier, A simple and effective method for separating meteorological from nonmeteorological targets using dual-polarization data. *J. Atmos. Ocean. Technol.* **35**, 1415–1424 (2018).
44. D. Mirkovic, P. M. Stepanian, J. F. Kelly, P. B. Chilson, Electromagnetic model reliably predicts radar scattering characteristics of airborne organisms. *Sci. Rep.* **6**, 35637 (2016).
45. D. Mirkovic, P. M. Stepanian, C. E. Wainwright, D. R. Reynolds, M. H. M. Menz, Characterizing animal anatomy and internal composition for electromagnetic modelling in radar entomology. *Remote Sens. Ecol. Conserv.* **5**, 169–179 (2019).
46. J. R. Coelho, Body temperature and flight muscle ratio in the burrowing mayfly, Hexagenia bilineata. *J. Freshw. Ecol.* **14**, 337–341 (1999).
47. S. O. Nelson, P. G. Bartley Jr., K. C. Lawrence, RF and microwave dielectric properties of stored-grain insects and their implications for potential insect control. *Trans. ASAE* **41**, 685–692 (1998).
48. M. A. Evans-White, R. S. Stelzer, G. A. Lamberti, Taxonomic and regional patterns in benthic macroinvertebrate elemental composition in streams. *Freshwater Biol.* **50**, 1786–1799 (2005).
49. S. Wright, W. M. Tidd, Summary of limnological investigations in western Lake Erie in 1929 and 1930. *Trans. Am. Fish. Soc.* **63**, 271–285 (1933).
50. V. E. Shelford, M. W. Boesel, Bottom animal communities of the island area of western Lake Erie in the summer of 1937. *Ohio J. Sci.* **42**, 179–190 (1942).
51. K. Wood, "Distribution and ecology of certain bottom-dwelling invertebrates of the western basin of Lake Erie," PhD thesis, The Ohio State University, Columbus, OH (1953).
52. N. W. Britt, Hexagenia (Ephemeroptera) population recovery in western Lake Erie following the 1953 catastrophe. *Ecology* **36**, 520–522 (1955).
53. J. F. Carr, J. K. Hiltunen, Changes in the bottom fauna of western Lake Erie from 1930 to 1961. *Limnol. Oceanogr.* **10**, 551–569 (1965).
54. US Department of Interior, "Lake Erie environmental summary 1963–1964" (Tech. Rep., Federal Water Pollution Control Administration, Cleveland, OH, 1968).
55. D. M. Veal, D. S. Osmond, "Bottom fauna of the western basin and near-shore Canadian waters of Lake Erie" in *Proceedings of the 11th Conference of Great Lakes Research* (International Association for Great Lakes Research, Ann Arbor, MI, 1968), pp. 151–160.
56. N. W. Britt, A. J. Pliodzinskas, E. M. Hair, "Benthic macroinvertebrate distribution in the central and western basins of Lake Erie" in *Lake Erie Nutrient Control Program*, C. Herdendorf, Ed. (USEPA, Duluth, MN, 1980).
57. R. Dermott, "Benthic invertebrate fauna of Lake Erie 1979: Distribution, abundance and biomass" (Tech. Rep., Great Lakes Laboratory for Fisheries and Aquatic Sciences, Canada Centre for Inland Waters, Burlington, ON, Canada, 1994).
58. OME, "An assessment of the bottom fauna and sediments of the western basin of Lake Erie, 1979" (Tech. Rep., Ontario Ministry of the Environment, London, ON, Canada, 1981).
59. B. A. Manny, D. W. Schloesser, *Changes in the Bottom Fauna of Western Lake Erie* (Backhuys Publishers, Leiden, the Netherlands, 1999), pp.197–217.
60. D. G. Farrara, A. J. Burt, "Environmental assessment of western Lake Erie sediments and benthic communities—1991" (Tech. Rep., Beak Consultants Limited, Brampton, ON, Canada, 1993).
61. E. L. Green, A. Grgicak-Mannion, J. J. H. Ciborowski, L. D. Corkum, Spatial and temporal variation in the distribution of burrowing mayfly nymphs (Ephemeroptera: Hexagenia limbata and H. rigida) in western Lake Erie. *J. Great Lakes Res.* **39**, 280–286 (2013).
62. J. Sauer, "Multiyear synthesis of the macroinvertebrate component from 1992 to 2002 for the long term resource monitoring program" (Tech. Rep. 2004-T005, US Geological Survey, Upper Midwest Environmental Sciences Center, La Crosse, WI, 2004).
63. M. J. Maccoux, A. Dove, S. M. Backus, D. M. Dolan, Total and soluble reactive phosphorus loadings to Lake Erie a detailed accounting by year, basin, country, and tributary. *J. Great Lakes Res.* **42**, 1151–1165 (2016).
64. E. M. Dean, "The effect of seasonal fish migration on energy budgets in two coastal Michigan streams," Master's thesis, Grand Valley State University, Allendale, MI (2016).
65. J. W. Nichols, C. P. Larsen, M. E. McDonald, G. J. Niemi, G. T. Ankley, Bioenergetics-based model for accumulation of polychlorinated biphenyls by nestling tree swallows, tachycineta bicolor. *Environ. Sci. Technol.* **29**, 604–612 (1995).